Available online at www.sciencedirect.com
ScienceDirect
Journal of Sound and Vibration 304 (2007) 894–917
JOURNAL OF SOUND AND VIBRATION
www.elsevier.com/locate/jsvi

Comparison of methods for parameter selection in Tikhonov regularization with application to inverse force determination

Hyoung Gil Choi[1], Anand N. Thite, David J. Thompson*

Institute of Sound and Vibration Research, University of Southampton, Highfield, Southampton SO17 1BJ, UK

Received 21 February 2006; received in revised form 22 March 2007; accepted 26 March 2007
Available online 15 May 2007

Abstract

In performing transfer path analysis of structure-borne sound transmission, the operational forces at the excitation points and/or at the connections within the structure-borne paths are required. These forces can be obtained by using inverse techniques but the measured data used will contain some unknown errors. Therefore the reconstructed forces may include large errors due to the inversion of an ill-conditioned matrix of these measured data. In this study, Tikhonov regularization is used in order to improve the conditioning of the matrix inversion. Several methods are available to select the optimal regularization parameter. The purpose of this paper is to compare the performance of the ordinary and generalized cross validation methods and the L-curve criterion. Simulations are carried out, representing measurements on a rectangular plate, for different noise levels in measured data. Also, the robustness of the conclusions is investigated by varying the shape of the plates, the force positions, and the noise levels included in the measured data. The L-curve method is found to perform better than OCV or GCV, particularly for high noise levels in the operational responses, but less well when these noise levels are low. It is therefore found to be less susceptible to producing large reconstruction errors but it tends to over-regularize the solution in the presence of low noise, leading to under-estimates of the forces. In practice, measurements of operational responses may be susceptible to noise contamination which suggests that the L-curve method is likely to be the most appropriate method in practical situations. Nevertheless, it is important to obtain good estimates of the likely noise in the signals before determining the most appropriate regularization technique. Ordinary cross validation method is generally found to have a better performance than generalized cross validation method if the matrix condition numbers are high. Since the need for regularization is greater with high condition numbers, it is consequently found that the ordinary cross validation method gives more reliable results overall than the generalized cross validation method.

1. Introduction

In performing transfer path analysis of structure-borne sound transmission, the operational forces at the excitation points or at the connections within the structure-borne paths are required. In the present application it is assumed, as is often the case, that the number of forces and their location are known. The

*Corresponding author. Tel.: +44 23 8059 2510; fax: +44 23 8059 3190.
E-mail address: djt@isvr.soton.ac.uk (D.J. Thompson).
[1]Current address: Mechatronics & Manufacturing Technology Center, Samsung Electronics Co., Ltd., 416 Maetan-3Dong, Yeongtong-Gu, Suwon 443-742, Korea.

0022-460X/$ - see front matter © 2007 Elsevier Ltd. All rights reserved.
doi:10.1016/j.jsv.2007.03.040

forces are difficult to measure directly so inverse techniques are often used, combining a measured frequency response function (FRF) matrix and a set of operational responses [1–4]. However such methods are sensitive to the conditioning of the FRF matrix, which has to be inverted. Since the measurements of the operational responses and the frequency response functions include some errors that cannot be known, the reconstructed forces and responses may contain large errors, magnified by the matrix inversion.

To reduce the errors caused by the inversion of the FRF matrix, the singular value rejection method has often been used in previous research [1–5]. This method usually results in reduced errors for the reconstructed forces. Verheij [1] described large (or compact) mechanical sources with uncorrelated (or correlated) equivalent point forces, which were estimated by the inverse method. In order to improve the conditioning of the matrix inversion, the singular value rejection method was introduced. Smaller singular values were rejected if they were corrupted by noise. A threshold to reject singular values was established based on estimates of the accelerance measurement errors. This equivalent forces method was then applied to studying sound transmission paths for a ship engine and gearbox [2]. Janssens et al. [3] applied this method to flanking paths of a diesel engine on a ship, in particular the drive shaft and cooling water pipes.

However, rejecting the singular values smaller than some threshold causes some information to be lost. A small change in the threshold can result in a singular value being accepted or rejected which may make a significant change to the results. To overcome this, the singular values can instead be weighted such as in Tikhonov regularization. Alternatively, the matrix inversion can be converted to a forward solution using an iterative process so that error amplification can be limited. Such a technique has been used extensively in digital image processing [6]. In this approach the iteration number determines the error amplification and its optimal value is determined based on estimates of bias and random errors in the solution.

Such methods of matrix regularization are often used to overcome ill-conditioning problems in other fields, such as Nearfield Acoustic Holography (NAH) [7,8] and acoustic source identification [9,10]. They have also been introduced more recently in inverse force determination [5,11,12]. In [12] it was shown that both Tikhonov regularization and the iterative inversion can improve the source reconstruction considerably, although the iterative technique involved considerable extra computational time whilst performing similarly to Tikhonov regularization.

In both techniques, it is important to choose an optimal value of regularization parameter or number of iterations. Thite [5,12] used ordinary cross validation (OCV) [13] for choosing an optimal value in Tikhonov regularization and also developed an alternative called selective cross validation. More recently it has been shown that regularization using OCV should be used where the matrix condition number is high but that results are better with no regularization where the condition number is low [14].

In the present paper, the techniques of generalized cross validation and L-curve criterion for selecting the optimal Tikhonov regularization parameter are considered and compared with OCV. Generalized cross validation (GCV) [15], is a rotation-invariant version of OCV. The L-curve is a plot of the norm of a regularized solution versus the norm of the corresponding residual as the regularization parameter is varied [16]. The shape of the curve is used in obtaining an optimal value for the regularization parameter. These methods have previously been applied for example to acoustic source identification problems [10,17]. Kim and Nelson especially compared the method of GCV and the L-curve method to determine the optimal regularization parameter for acoustic source reconstruction [17]. They concluded that L-curve is most effective when the problem is relatively well-conditioned and the reconstruction result is mainly dominated by contaminating noise whereas GCV provides a more reasonable amount of regularization for ill-conditioned problems where the noise levels are relatively low.

The purpose of the present study is to compare the performance of the methods of GCV and L-curve with that of OCV for inverse force determination. To achieve this use is made of simulations on a simple structure; as in [5,11,12] a flat rectangular plate is used.

Although the use of simulations may have limitations, inevitably involving an arbitrary choice of contaminating noise, it has the advantage over measurements that the correct answer is known a priori, allowing more detailed comparisons of the performance of the methods. Moreover, it readily allows consideration of a large number of variants. In contrast, for measured data, the correct answer is not known reliably, nor can the noise contamination be determined precisely. Therefore, no results are presented here for measured data, as these would not allow sufficient discrimination between the methods to be useful.

Structural applications differ from the acoustic one (e.g. [10,17]) in the respect that the transfer functions tend to be much more strongly resonant. Although the results presented are limited to a flat rectangular plate, there is nothing inherent in this structure that affects the conclusions, which are presented in terms of matrix condition numbers and signal-to-noise (S/N) ratios. It is therefore expected that the conclusions are, at least qualitatively, applicable more generally to force identification on other structures.

The robustness of each of these methods is assessed for different noise levels and under the variation of a number of parameters. The parameters varied are the shape of the plates, the force positions (the relationship among force positions themselves and the relationship between force and response positions) and the noise levels included in measured FRFs and operational responses. Considering these factors, the performance of OCV, GCV and L-curve is compared in terms of the average errors in the reconstructed forces.

2. Methods for selecting the Tikhonov regularization parameter

2.1. Tikhonov regularization

It is supposed that a vector of operational responses $\hat{a}$ are measured at some positions, and that the matrix of frequency response functions $\hat{A}$ from a set of force positions to the above response positions are also measured. The force positions are assumed to be known. The objective is to find a vector of forces $\tilde{F}$ such that $\hat{a} \cong \hat{A}\tilde{F}$.

The measured operational responses $\hat{a}$ and the measured frequency response functions $\hat{A}$ contain some errors that are unknown. Therefore, if it is supposed that the fitted force $\tilde{F}$ can be obtained, a fitting error can be defined as

$$\tilde{e} = \hat{a} - \hat{A}\tilde{F}. \tag{1}$$

To minimize such fitting errors $\tilde{e}$, Tikhonov suggested a cost function given by

$$J = (\tilde{e}^H \tilde{e}) + \lambda(\tilde{F}^H \tilde{F}), \tag{2}$$

or

$$J = (\hat{a} - \hat{A}\tilde{F})^H(\hat{a} - \hat{A}\tilde{F}) + \lambda(\tilde{F}^H \tilde{F}), \tag{3}$$

where λ is a regularization parameter and H indicates Hermitian transpose. For this cost function to be minimized, the first derivative of J with respect to the force vector $\tilde{F}$ must be zero. The optimal solution to minimize the error amplification in force reconstruction is found to be

$$\tilde{F} = (\hat{A}^H \hat{A} + \lambda I)^{-1} \hat{A}^H \hat{a}. \tag{4}$$

Using the singular value decomposition of the accelerance matrix, $\hat{A} = USV^H$, in which S is a diagonal matrix of singular values and U and V are unitary matrices, Eq. (4) can be represented as

$$\tilde{F} = V(S^H S + \lambda I)^{-1} S^H U^H \hat{a}. \tag{5}$$

Thus the singular value s_i becomes $s_i/(s_i^2 + \lambda)$ in the regularized inverse.

Now the problem is how to select an appropriate regularization parameter λ to obtain the optimal force vector. To do this, it is necessary to know the errors in the measurement but, as previously stated, the errors are unknown. Consequently several kinds of mathematical concept that approximate the errors are used, for example, ordinary cross validation, generalized cross validation, etc. In the next sections, these methods are presented briefly.

2.2. Ordinary cross validation

In the method of ordinary cross validation [13], the force vector $\tilde{F}_k$ is determined by using Eq. (5) with the measured operational responses except one (the kth). The kth response is reconstructed by using the force vector $\tilde{F}_k$ multiplied by $\hat{A}_k$, the vector containing the kth column of $\hat{A}$. The difference is calculated between the

kth measured operational response $\hat{a}_k$ and this estimate $\hat{A}_k\tilde{F}_k$. Hence the ordinary cross validation function is defined as

$$V_O(\lambda) = \frac{1}{m}\sum_{k=1}^{m}\left|\hat{a}_k - \hat{A}_k\tilde{F}_k\right|^2, \tag{6}$$

where m is the number of responses. Eq. (6) can be rewritten in matrix form as [15]:

$$V_O(\lambda) = \frac{1}{m}\left\|B(\lambda)(I - C(\lambda))\hat{a}\right\|^2, \tag{7}$$

where $\|\cdot\|$ indicates the Euclidean norm, $C(\lambda) = \hat{A}(\hat{A}^H\hat{A} + \lambda I)^{-1}\hat{A}^H$ and $B(\lambda)$ is the diagonal matrix whose entries are given by $1/(1 - c_{kk}(\lambda))$, $c_{kk}(\lambda)$ being the kth diagonal entry of $C(\lambda)$.

For a series of values of the regularization parameter, the cross validation function $V_O(\lambda)$ is calculated and the value of λ that corresponds to the minimum of $V_O(\lambda)$ is identified as the optimal value of regularization parameter. Using the optimal value of λ, the optimal forces and responses can be reconstructed using the full matrix $\hat{A}$. This process is carried out for each frequency.

2.3. Generalized cross validation

In the extreme case where the entries of the measured frequency response functions $\hat{A}$ are 0 except for the jjth entries ($j = 1, 2, \ldots, m$), the matrix $C(\lambda)$ in Eq. (7) is diagonal, and consequently:

$$V_O(\lambda) = \frac{1}{m}\|\hat{a}\|^2 = \frac{1}{m}\sum_{k=1}^{m}|\hat{a}_k|^2. \tag{8}$$

In other words the force determining a_k is found to be 0 when a_k is omitted from $\hat{A}$, and so the reconstructed a_k is zero. In this case, the ordinary cross validation function is independent of the choice of the regularization parameter so that the method of ordinary cross validation would not perform very well in such near-diagonal cases. Golub et al. [15] therefore suggested a modification to the method called generalized cross validation, which follows from the argument that any good choice of λ should be invariant under rotation of the measurement coordinate system. Generalized cross validation is thus a rotation-invariant form of ordinary cross validation. This method may be derived as follows.

First, a matrix W is defined as a unitary matrix that diagonalizes the circulant matrices. The entries of this matrix are given by

$$W_{jk} = \frac{1}{\sqrt{m}}e^{2\pi i(jk/m)}, \quad j, k = 1, 2, \ldots, m, \tag{9}$$

where m is the number of response positions. Multiplying a matrix by W has the effect of applying a discrete Fourier transform to this matrix. It will be used for resolving the diagonal problem of the measured frequency response functions.

Next, using the singular value decomposition of the measured frequency response function $\hat{A}$, Eq. (1) can be written as

$$\tilde{e} = \hat{a} - USV^H\tilde{F}. \tag{10}$$

If this is pre-multiplied by U^H and then by W this gives

$$WU^H\tilde{e} = WU^H\hat{a} - WSV^H\tilde{F}. \tag{11}$$

This transformed model is represented as

$$\tilde{e}_t = \hat{a}_t - \hat{A}_t\tilde{F}, \tag{12}$$

where $\hat{a}_t = WU^H\hat{a}$ is the vector of transformed measured operational responses, $\hat{A}_t = WSV^H$ the vector of transformed frequency response functions, and $\tilde{e}_t = WU^H\tilde{e}$ the vector of transformed fitted errors.

By applying ordinary cross validation to this transformed model, Eq. (12), the generalized cross validation function can be defined as

$$V_G(\lambda) = \frac{(1/m)\left\|(I - C_t(\lambda))\hat{a}_t\right\|^2}{[(1/m)\mathrm{Tr}(I - C_t(\lambda))]^2}, \tag{13}$$

where $C_t(\lambda) = \hat{A}_t(\hat{A}_t^H \hat{A}_t + \lambda I)^{-1}\hat{A}_t^H$ is a circulant matrix and thus constant along the diagonals. Since $C(\lambda)$ and $C_t(\lambda)$ have the same eigenvalues, Eq. (13) can be written as

$$V_G(\lambda) = \frac{(1/m)\left\|(I - C(\lambda))\hat{a}\right\|^2}{[(1/m)\mathrm{Tr}(I - C(\lambda))]^2}. \tag{14}$$

Furthermore, it can also be shown [15] that $V_G(\lambda)$ is a weighted version of the ordinary cross validation function $V_O(\lambda)$ so that

$$V_G(\lambda) = \frac{1}{m}\sum_{k=1}^{m}\left|\hat{a}_k - \hat{A}_k\tilde{F}_k\right|^2 w_k, \tag{15}$$

where $w_k = [1 - c_{kk}/(1 - (1/m)\mathrm{Tr}C(\lambda))]^2$.

2.4. L-curve criterion

The L-curve [16] is a log–log plot of the norm of a regularized solution versus the norm of the corresponding residual (fitting error) as the regularization parameter is varied. It is a convenient graphical tool for displaying the trade-off between the size of the regularized reconstructed forces and the fit to the given response data. Here the norm of the reconstructed forces $\left\|\tilde{F}\right\|$ is plotted against norm of the residue $\left\|(\hat{a} - \hat{A}\tilde{F})\right\|$. As the regularization parameter λ increases, the norm of the reconstructed forces $\left\|\tilde{F}\right\|$ decreases monotonically and the norm of the residue increases monotonically. The curve is L-shaped: approximately vertical for small λ, and approximately horizontal for large λ, with the corner providing the optimal regularization parameter. In other words, the rationale behind this choice is that the corner separates the flat and vertical parts of the curve, where the solution is dominated by regularization errors and random errors, respectively. It is suggested [16] that the point on the L-curve that has maximum curvature should be chosen as corner of the curve and therefore the optimal parameter value. This can therefore be automated without the need to plot the L-curves.

3. Simulations

3.1. Analysis object

To compare the effectiveness of OCV, GCV and L-curve, a series of numerical simulations have been carried out based on a simply supported rectangular plate. Numerical simulations have the advantage that a correct answer is known, allowing the methods to be assessed more fully than with measured data.

As in Refs. [5,11,12] the plate is taken to have dimensions $600 \times 500 \times 1.5$ mm and its material is steel (Young's modulus: 2.07×10^{11} N/m^2, Poisson's ratio: 0.3, density: 7850 kg/m^3, and damping loss factor: 0.03). Four positions were selected at random for applying coherent point forces perpendicular to the plate, and five positions for measuring operational responses. This 5×4 case is small enough that the use of regularization is necessary [14]. One more response than force is needed for the cross validation process. The locations of the force and response measurement positions are shown in Table 1. The forces are defined in terms of their frequency spectra: they are chosen to have broad-band spectra with constant rms amplitudes in each one-third octave band (i.e. 'pink' noise). The corresponding amplitudes are listed in the table.

The frequency range used initially for the simulations is from 10 Hz to 3.6 kHz. The plate response is dominated by individual modes at low frequencies and by multiple overlapping modes at high frequencies. The first mode occurs at 25 Hz. A typical frequency response function is given in Fig. 1.

Table 1
Non-dimensional positions of forces and responses

Force positions and rms amplitude				Response positions		
No	x/a	y/b	Force (N)	No	x/a	y/b
1	0.41	0.43	19.0	1	0.55	0.40
2	0.51	0.63	10.0	2	0.90	0.80
3	0.62	0.41	27.0	3	0.60	0.50
4	0.31	0.72	6.0	4	0.70	0.71
				5	0.61	0.31

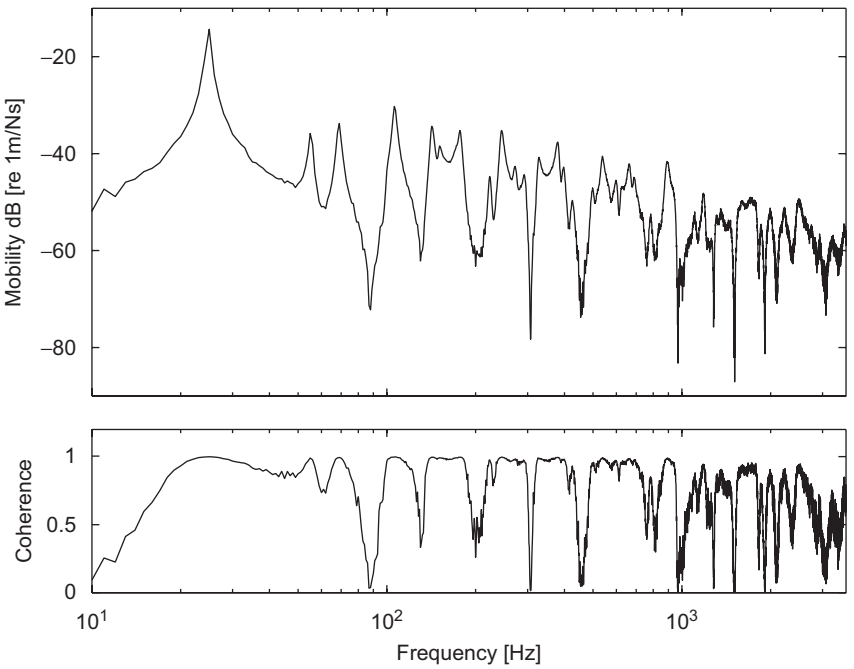

Fig. 1. Transfer mobility from excitation point 3 to response point 1 for high noise.

Table 2
Average signal-to-noise ratios in dB of operational responses and FRFs and average condition number of FRFs

		Noise levels		
		Low (high S/N)	Medium (medium S/N)	High (low S/N)
Operational response (dB)		50.0	13.5	2.6
FRF	Acceleration (dB)	49.0	27.3	11.3
	Force (dB)	60.0	40.0	32.0
	Condition number	46.8	17.2	12.2

In these simulations, noise signals should be added to the 'measured' signals because an analytical model would otherwise have an exact solution allowing inversion without any errors. The so-called measurement noise was added to the acceleration and force signals [5]. The noise levels added to obtain operational responses and frequency response functions can be quantified by the average S/N ratio across all one-third octave bands and are classified as low, medium and high. These average values for the three levels of noise

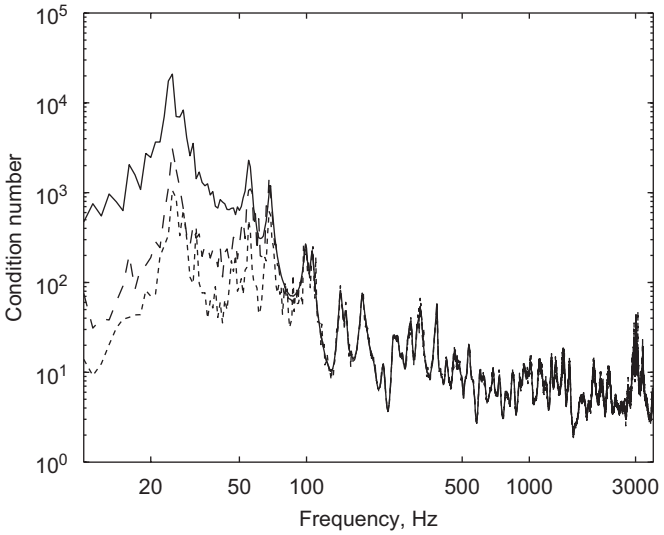

Fig. 2. Condition numbers of the measured frequency response functions due to different levels of noise: —— low noise level, – – – medium, ------ high.

used are shown in Table 2, although note that the S/N ratio actually varies with frequency [5]. In modelling the noise an arbitrary choice has to be made as it is not feasible to consider every type of noise.

The numbers of averages that have been used in estimating FRFs and operational responses are 50 and 25, respectively.

The condition numbers of the measured frequency response functions in the presence of different noise levels are shown in Fig. 2 and the frequency averaged condition number is also given in Table 2. The highest peak at 25 Hz corresponds to the first mode of the plate and is highest for low noise in the FRFs.

3.2. Force determination

Examples of the forces determined by using the three methods of OCV, GCV and L-curve are shown in Fig. 3. The noise levels in the measurements here correspond to low noise in the FRFs and medium noise in the responses. This case is chosen because in Ref. [5] it was found to be particularly difficult to obtain good results, especially at low frequency where the condition number is high. All results are calculated in narrow bands (1 Hz spacing) and the results are converted to one-third octave bands for presentation. The true forces applied for all frequency bands are shown in the right-hand part of the figure (constant for each frequency band). The forces are predicted more reliably at high frequencies than at low frequencies, and are better for the larger forces than the smaller ones. At low frequencies, large force determination errors result from high condition numbers (Fig. 2).

For the simulation considered, the forces reconstructed using Tikhonov regularization with OCV are more reliable than with GCV below 100 Hz. Using the L-curve method reduces error amplification at low frequencies, but in most cases over-regularizes the solution leading to under-estimates of the forces. At higher frequencies all three methods reconstruct the forces equally well.

3.3. Robustness for different noise levels

To investigate the robustness of each method in selecting the regularization parameter for different levels of noise in the responses and the FRFs, calculations are performed for the various combinations of noise level identified in Table 2. As well as ordinary cross validation, generalized cross validation and L-curve, a fourth, idealized method of determining the regularization parameter is considered for comparison. This, referred to as minimum force error (MFE), uses the fact that the forces are known to find the value of regularization parameter that minimizes the force error. The mean-square error in the forces over all frequencies is

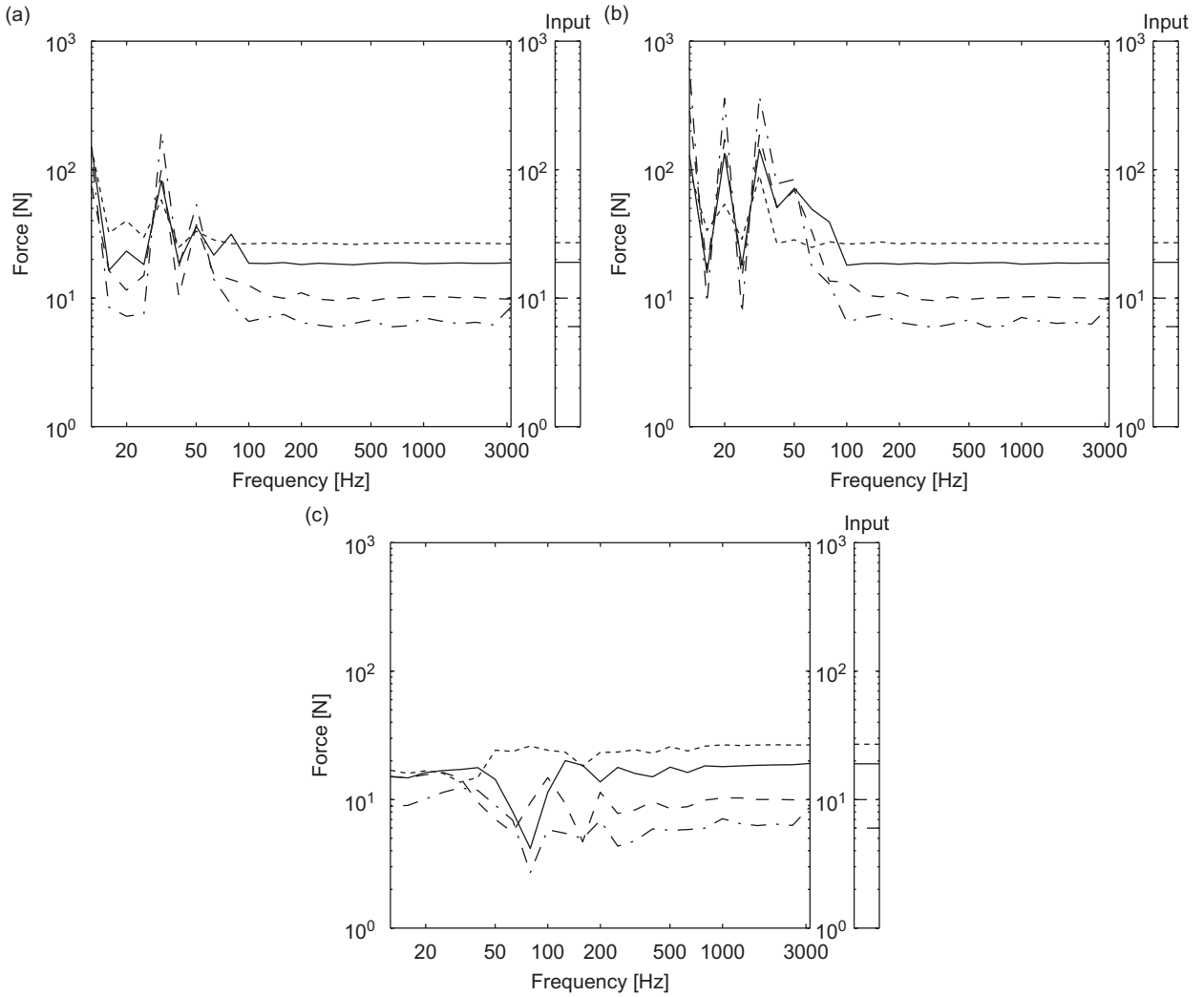

Fig. 3. Reconstructed rms forces in one-third octave bands using low noise in accelerances and medium noise in the responses: —— force 1, – – – force 2, ------ force 3, –·–·– force 4. (a) OCV; (b) GCV; and (c) L-curve.

determined for a range of values of regularization parameter and the value that yields the minimum such force error is selected. This represents an ideal case and shows the best that could be achieved by regularization; *it is not intended as a practical method*. The MFE does not result in zero force error due to the presence of noise contamination; it gives an indication of the error amplification due to the ill-conditioning of the FRF matrix.

To select the optimal regularization parameter for each method, the corresponding validation function V is evaluated initially for a wide range of regularization parameters, given by $\lambda = 0$, $s_{\max}^2 \times \{10^{-10}, \ldots, 1\}$ where $s_{\max}$ is the largest singular value and the values except 0 are spaced logarithmically (50 points per decade).

To simplify the presentation an average error estimate is used, given as follows:

$$\varepsilon_{\text{force}} = \frac{1}{n}\sum_{j=1}^{n}\left[\frac{1}{N}\sum_{k=1}^{N}\left|L_{\tilde{F},j} - L_{F,j}\right|_k^2\right]^{1/2}, \tag{16}$$

where $\varepsilon_{\text{force}}$ is the average force error in dB, n is the number of force positions, N is the number of one-third octave bands k in the frequency range considered, $L_{\tilde{F},j}$ is the reconstructed jth force level in one-third octave

Table 3
Average errors in dB calculated in one-third octave bands in forces reconstructed in the frequency range of 10–500 Hz for the initial plate

		Noise levels in operational responses		
		Low	Medium	High
OCV				
Noise levels in FRFs	Low	1.8	9.6	13.4
	Medium	2.7	4.2	9.5
	High	2.6	3.3	4.7
GCV				
Noise levels in FRFs	Low	1.6	10.5	17.3
	Medium	2.7	4.9	11.6
	High	2.7	3.4	6.4
L-curve				
Noise levels in FRFs	Low	4.0	3.9	2.9
	Medium	4.2	4.0	3.2
	High	4.1	4.0	3.4
MFE				
Noise levels in FRFs	Low	0.4	1.4	2.2
	Medium	1.3	1.5	2.3
	High	2.0	2.0	2.4

bands in dB and $L_{F,j}$ is the actual force level in one-third octave bands in dB. These are evaluated over the limited frequency range 10–500 Hz as the errors in the reconstructed forces are small at higher frequency, see Fig. 3.

Table 3 shows the results. For the methods of OCV and GCV, the inverse force determination is observed to be very sensitive to the noise level in the response when the condition numbers are large (i.e. low FRF error). The forces determined by GCV are a little worse on average than those found by OCV, probably because, for the case considered, the FRF matrix is not near-diagonal. The L-curve method gives much improved estimation of forces for high noise in operational responses but the results are inferior to OCV for low noise in operational responses. The average errors obtained by the L-curve method are largely independent of the noise levels.

Not surprisingly all the results are worse than the ideal case, MFE. However, it is interesting to note that the average errors of forces obtained by MFE increase as the noise levels increase, not only those in the FRFs but also those in the operational responses. By contrast, the average errors of forces reconstructed by OCV and GCV are largest for high noise levels in the operational responses and low noise levels in the FRFs, where the condition numbers are highest (Fig. 2).

Fig. 4 shows the regularization parameters chosen to minimize the ordinary cross validation function for low/high noise levels in FRFs and low/high noise levels in operational responses. When zero values are selected for λ, these are shown along the bottom of the graph. Also shown in each case are the maximum squared singular value, $s^2_{\max}$, 10^{-10} times this, the minimum squared singular value, $s^2_{\min}$, and the square of the error norm $\|E\|^2$ of the matrix $\hat{A}$. This gives an indication of the form of the added noise spectrum. It can be seen that larger regularization parameters are selected as the noise levels in FRFs and/or in operational responses increase. It is observed that the selected regularization parameter generally increases as the frequency increases (in proportion to the square of the largest singular value).

Fig. 5 shows, for each method, the regularization parameters chosen to minimize the corresponding validation function. These results correspond to low noise in the FRFs and medium noise in the operational responses, as in Fig. 3. In Fig. 5, the trends of the results from OCV, GCV and MFE are similar although GCV never selects a zero value for λ. The L-curve criterion selects a regularization parameter that varies very smoothly with frequency but which is generally higher than the other methods at low frequencies.

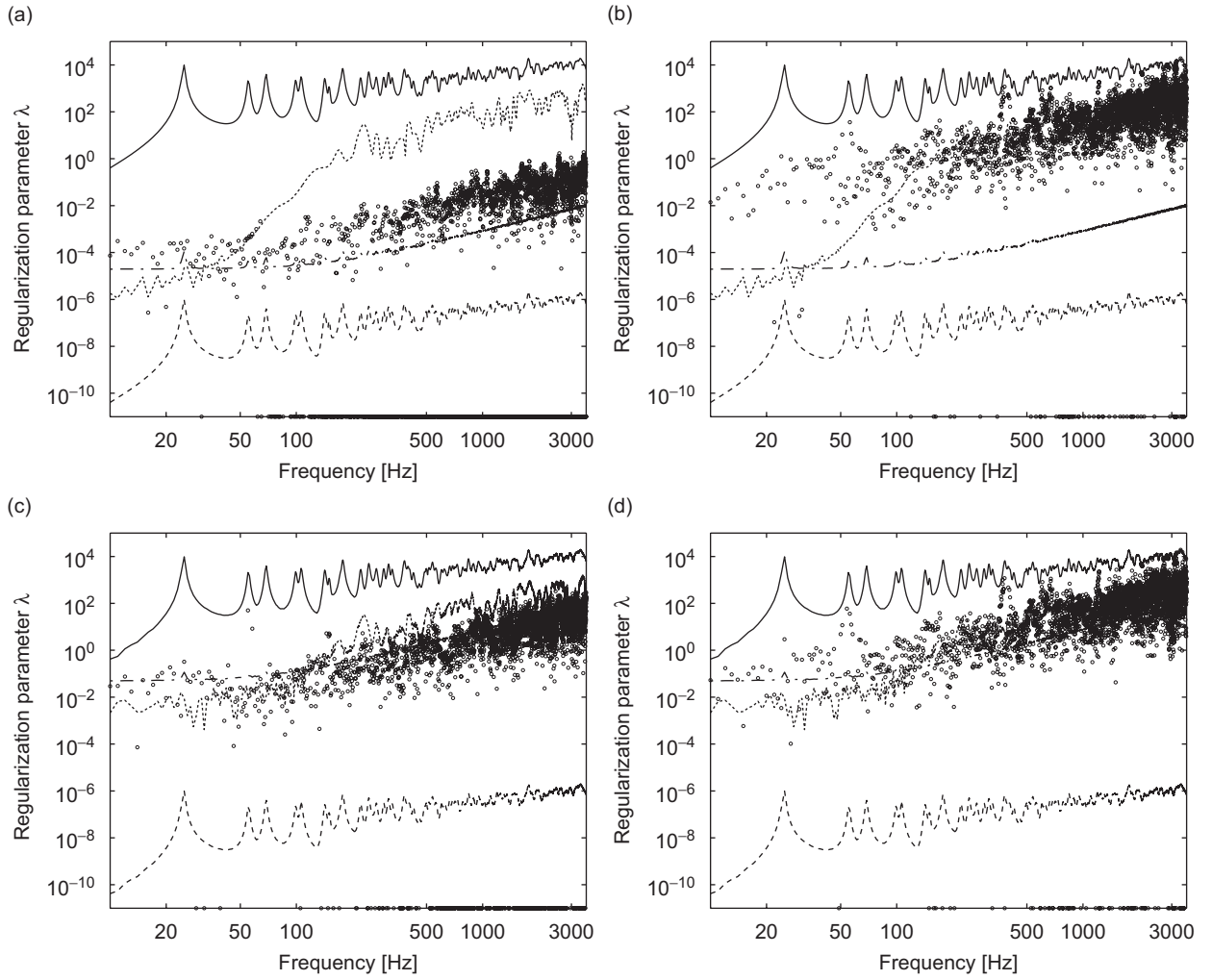

Fig. 4. Regularization parameters chosen by the method of ordinary cross validation for different noise levels (○). —— $s^2_{\max}$, – – – $10^{-10} \times s^2_{\max}$, ------ $s^2_{\min}$, –·–·– $\|E\|^2$. (a) Low resp. noise, low FRF noise; (b) high resp. noise, low FRF noise; (c) low resp. noise, high FRF noise; and (d) high resp. noise, high FRF noise.

4. Effect of the dimensions of the plate

In the previous section, the method of ordinary cross validation was found generally to give better results than the method of generalized cross validation. The L-curve method gave much better results in the presence of high noise in the responses but worse results with low noise. To extend confidence in these conclusions, the effects of varying a number of parameters on the performance of the methods of OCV, GCV and L-curve are investigated in this and the following sections. These parameters are the shape (the dimensions) of the plate, the positions of the forces applied, and the S/N ratios in the FRFs and the operational responses.

Different shapes of plate are studied as this affects the modal distribution with frequency and hence the condition numbers. As well as the rectangle with an aspect ratio of 6:5 considered above, a square, and a strip with an aspect ratio of about 1:5 (actually 100:511) are considered. All three have the same area, so the corresponding dimensions are $0.6 \times 0.5\,\text{m}$, $0.548 \times 0.548\,\text{m}$, and $0.242 \times 1.238\,\text{m}$, respectively. The non-dimensional positions of forces and responses are the same as those for the initial rectangular plate (Table 1). All other parameters and conditions are kept the same.

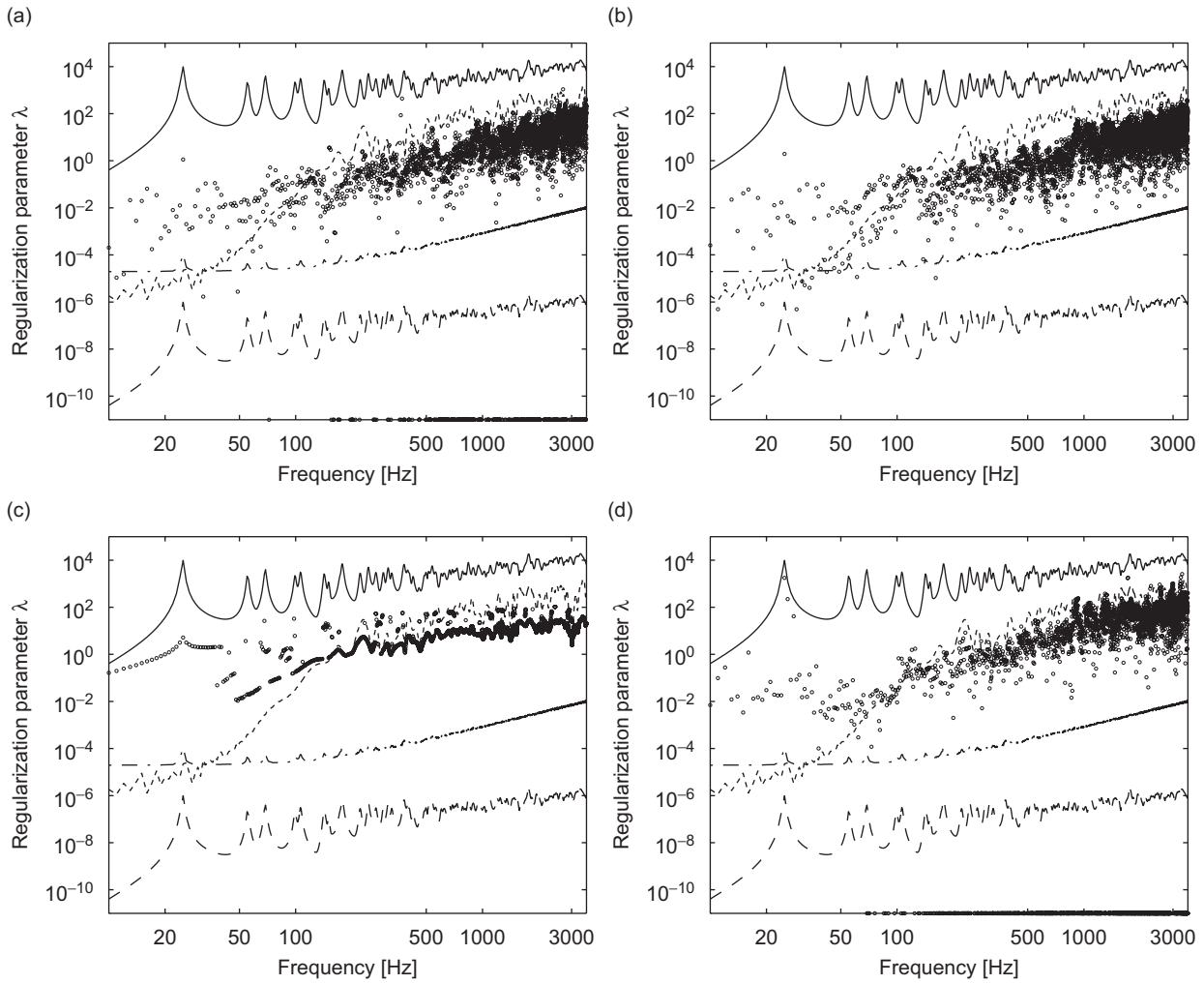

Fig. 5. Selected regularization parameters for low noise level in FRFs and medium noise level in operational responses (○). —— s^2_{max}, – – – $10^{-10} \times s^2_{max}$, ------ s^2_{min}, –·–·– $\|E\|^2$. (a) OCV; (b) GCV; (c) L-curve; and (d) MFE.

The frequency range used is again limited to 10–500 Hz because the results obtained by all three methods are similar to each other above 500 Hz. Three noise levels in the operational responses and FRFs are used, which are the same as those used in the previous section.

Table 4 shows the average errors in reconstructed forces for the square plate. The condition numbers are shown in Fig. 6. In comparison with the results of the rectangular plate, the average errors in forces reconstructed by OCV and GCV generally reduce by about 1–4 dB, except in the case of high noise level in FRFs, because the condition numbers become smaller in the case of low/medium noise levels in FRFs. Therefore, since the differences between the average errors found by OCV and by GCV decrease, especially for high noise level in operational responses, OCV and GCV show more similar results. Nevertheless OCV mostly gives better results than GCV. There is very little change in the results of the L-curve method compared with the rectangular plate, as the selection here appears to be less sensitive to condition numbers.

For the strip plate, the average errors in reconstructed forces are shown in Table 5. Due to its large aspect ratio, this plate has a higher first natural frequency than the others (65 Hz) but subsequent modes occur close together in frequency, and its mode shapes are essentially one dimensional below 250 Hz. These features have the effect of reducing the condition numbers, as shown in Fig. 7. The average force errors for the strip plate are

Table 4
Average errors in dB calculated in one-third octave bands in forces reconstructed in the frequency range of 10–500 Hz for the square plate

		Noise levels in operational responses		
		Low	Medium	High
OCV				
Noise levels in FRFs	Low	1.0	5.1	12.8
	Medium	1.7	4.0	6.1
	High	3.4	3.3	4.5
GCV				
Noise levels in FRFs	Low	1.2	6.2	14.3
	Medium	2.7	4.7	7.8
	High	3.4	3.9	5.2
L-curve				
Noise levels in FRFs	Low	3.9	3.6	3.2
	Medium	3.9	3.7	3.3
	High	3.8	3.6	3.6
MFE				
Noise levels in FRFs	Low	0.3	1.3	2.0
	Medium	1.1	1.6	2.2
	High	2.1	2.0	2.4

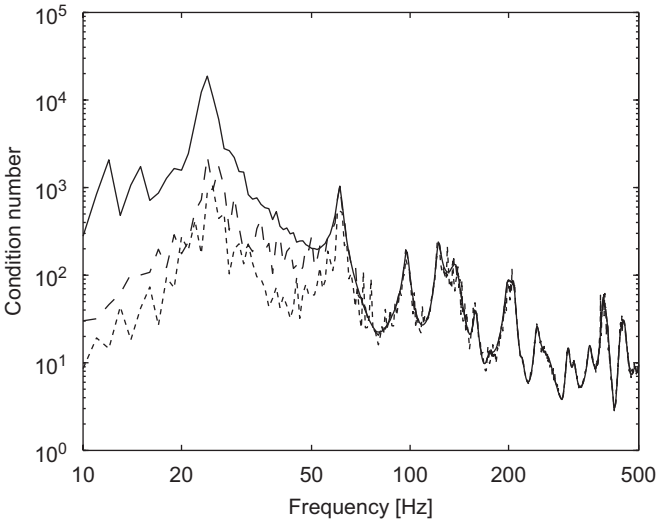

Fig. 6. Condition numbers of the measured FRFs due to different levels of noise for the square plate: —— low noise level, – – – medium, ------ high.

smaller than those for the other plates, particularly for OCV and GCV because of the reduction in the condition numbers. However the differences between the results for OCV and by GCV are larger than for the other plates, especially in the cases of medium/high noise levels in operational responses and low/medium noise levels in FRFs. Therefore in this case, OCV is more clearly superior to GCV. As far as the L-curve is concerned very little change is seen from the earlier two cases, although some improvement is seen for low response noise.

Table 5
Average errors in dB calculated in one-third octave bands in forces reconstructed in the frequency range of 10–500 Hz for the strip plate

		Noise levels in operational responses		
		Low	Medium	High
OCV				
Noise levels in FRFs	Low	0.8	3.5	10.3
	Medium	1.7	2.8	4.9
	High	2.4	3.2	4.5
GCV				
Noise levels in FRFs	Low	0.8	8.9	12.9
	Medium	1.5	4.5	10.4
	High	2.4	3.4	5.7
L-curve				
Noise levels in FRFs	Low	4.9	2.3	3.8
	Medium	2.0	2.1	2.8
	High	3.2	3.2	2.6
MFE				
Noise levels in FRFs	Low	0.3	1.5	1.8
	Medium	0.8	1.3	1.9
	High	1.5	1.7	2.0

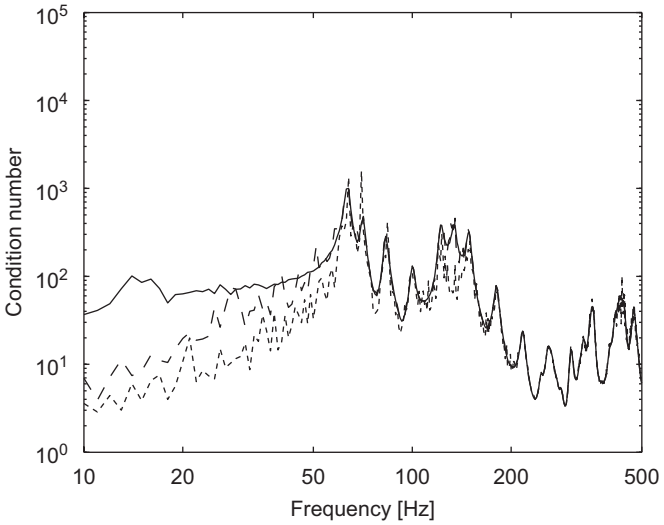

Fig. 7. Condition numbers of the measured FRFs due to different levels of noise for the strip plate: —— low noise level, – – – medium, ------ high.

5. Effect of the distribution of applied force locations

In order to determine whether the conclusions reached are dependent on the choice of force and response positions, four different distributions of force positions were used and their results were compared. The four distributions are as follows:

(1) Initial distribution of force positions,
(2) A distribution of force positions close to one another,

(3) A distribution of force positions far from one another,
(4) A distribution of force positions near to the response positions.

Fig. 8 shows the non-dimensional positions of forces mentioned above and the response positions.

A distribution of force positions close to one another is obtained by choosing four points randomly within a circle of non-dimensional diameter 0.1, see Fig. 8(b). It is expected that the condition number will be much higher at low frequencies as the FRFs corresponding to each force position are very similar. The condition numbers of the FRF matrices are shown in Fig. 9.

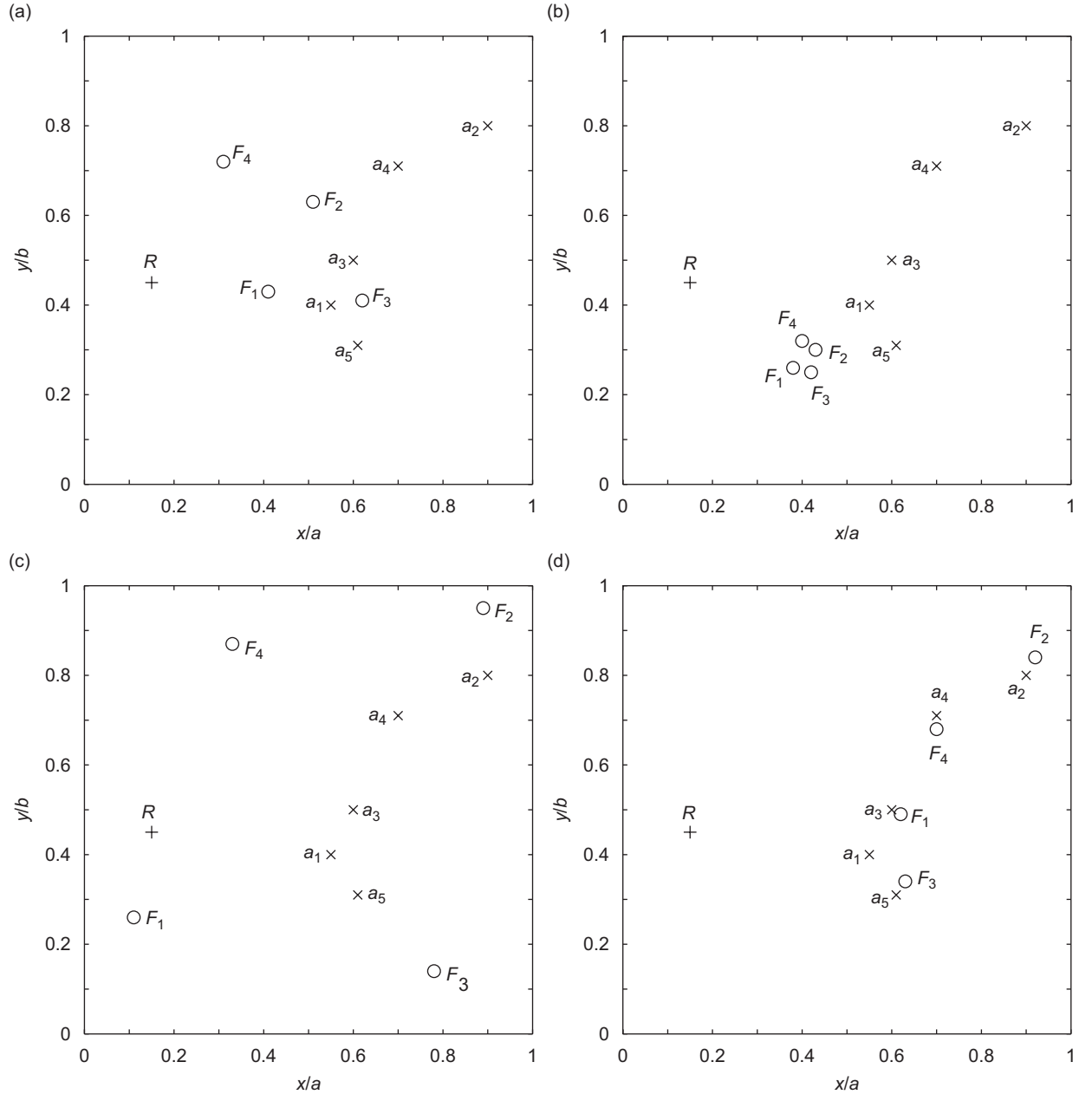

Fig. 8. Various positions of forces. ○: force location, ×: response location, +: receiver location. (a) Initial distribution; (b) close distribution; (c) far distribution; and (d) near to response positions.

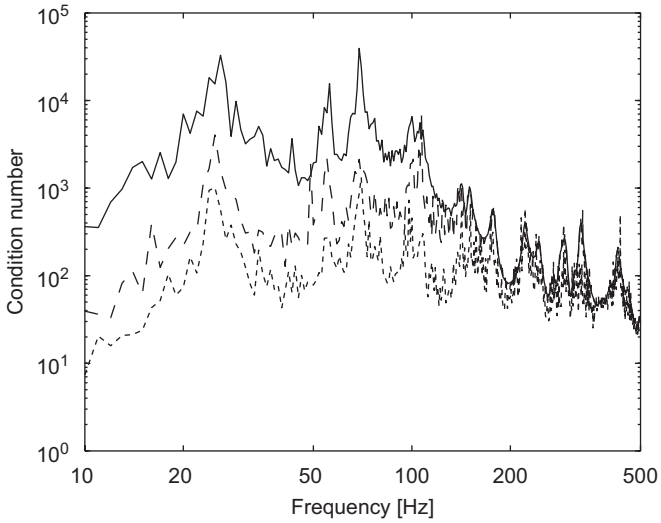

Fig. 9. Condition numbers of the measured FRFs due to different levels of noise for the close distribution of forces: —— low noise level, – – – medium, ------ high.

Table 6
Average errors in dB calculated in one-third octave bands in forces reconstructed in the frequency range of 10–500 Hz for the close distribution of force positions

		Noise levels in operational responses		
		Low	Medium	High
OCV				
Noise levels in FRFs	Low	1.9	14.3	22.3
	Medium	4.1	6.5	12.8
	High	4.2	4.9	7.5
GCV				
Noise levels in FRFs	Low	2.2	17.6	29.8
	Medium	4.1	7.8	14.8
	High	4.3	5.1	7.9
L-curve				
Noise levels in FRFs	Low	4.0	4.1	4.6
	Medium	4.3	4.3	4.6
	High	4.2	4.2	4.6
MFE				
Noise levels in FRFs	Low	1.5	3.1	3.3
	Medium	3.2	3.1	3.4
	High	3.3	3.4	3.4

The average errors in reconstructed forces are given in Table 6. Force errors become larger than those obtained from the initial distribution (Table 3) because of the increase in the condition numbers of the FRF matrices. In this case OCV gives force estimates better than or equal to GCV for each noise level. Even in this situation, the error levels for the L-curve method are very similar to those for the initial distribution of forces (Table 3), and only increase a little for high response noise.

To create a distribution of force positions far from one another four points were selected randomly, such that they were each at least a non-dimensional distance 0.5 from one another, as shown in Fig. 8(c). The condition numbers are plotted in Fig. 10 and can be seen to have reduced considerably at low frequencies as the FRFs become much less inter-dependent.

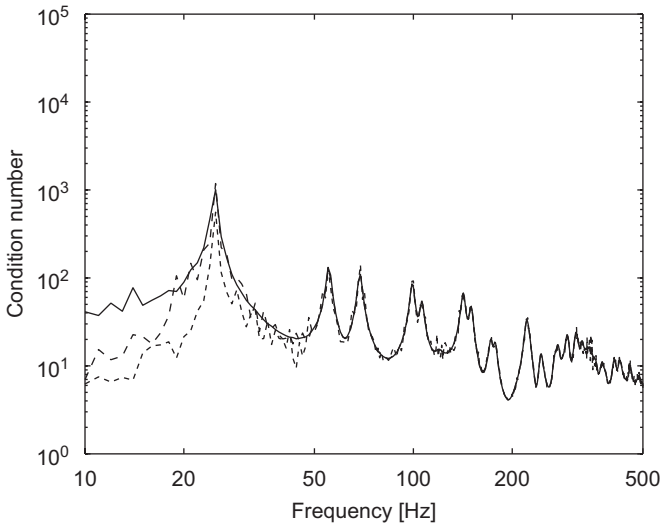

Fig. 10. Condition numbers of the measured FRFs due to different levels of noise for the far distribution of forces: —— low noise level, – – – medium, ------ high.

Table 7
Average errors in dB calculated in one-third octave bands in forces reconstructed in the frequency range of 10–500 Hz for the far distribution of force positions

		Noise levels in operational responses		
		Low	Medium	High
OCV				
Noise levels in FRFs	Low	0.8	5.2	7.4
	Medium	2.9	4.0	4.9
	High	2.9	2.9	5.6
GCV				
Noise levels in FRFs	Low	0.9	6.2	7.6
	Medium	2.9	5.0	5.4
	High	2.7	3.0	6.2
L-curve				
Noise levels in FRFs	Low	6.5	6.1	4.8
	Medium	6.0	5.4	4.6
	High	5.5	5.4	4.5
MFE				
Noise levels in FRFs	Low	0.5	2.1	2.7
	Medium	1.7	1.9	2.5
	High	2.1	2.3	2.7

Table 7 gives the average errors in reconstructed forces. Comparing these results with those of the original and close distributions, there are smaller force errors for OCV and GCV at low noise levels in FRFs, due to the reduction in the condition numbers. However, for the L-curve method the errors become larger for low and medium noise in responses. Overall, the differences between OCV and GCV are smaller in this case, but the results for OCV remain slightly better than for GCV. OCV gives better results than L-curve here for medium as well as low noise in responses.

A distribution of force positions close to the response points is made by generating points randomly within a radius of 0.05 for each response point. The 1st, 2nd, 3rd and 4th force positions are near to the 3rd, 2nd, 5th and 4th response positions, respectively, see Fig. 8(d). The condition numbers are given in Fig. 11. They can be seen to be

reduced considerably for low and medium noise levels, but for high noise level in the FRFs the condition numbers are similar to those of the original distribution. They are consequently much less sensitive to noise in the FRFs.

Table 8 shows the results of the average errors in reconstructed forces. Comparing these results with those in the original case (Table 3) for OCV and GCV, the force errors for low and medium noise levels in FRFs decrease considerably. The errors in the forces are generally lower here than for the far distribution, although condition numbers are similar. This can be attributed to the fact that the FRF matrix is closer to 'diagonal', i.e. strongly dominated by one term in each row.

In the present case OCV still generally gives better results than GCV although the differences are small despite the matrix being near-diagonal. The L-curve gives better results here than for the far distribution of

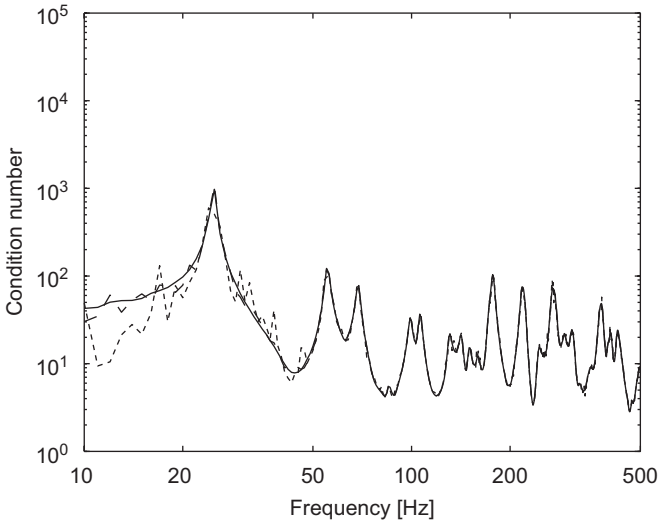

Fig. 11. Condition numbers of the measured FRFs due to different levels of noise for the distribution of force positions near to response positions: —— low noise level, – – – medium, ------ high.

Table 8
Average errors in dB calculated in one-third octave bands in forces reconstructed in the frequency range of 10–500 Hz for the distribution of force positions near to response positions

		Noise levels in operational responses		
		Low	Medium	High
OCV				
Noise levels in FRFs	Low	0.2	2.9	6.1
	Medium	1.5	2.4	6.9
	High	2.8	3.2	3.2
GCV				
Noise levels in FRFs	Low	0.2	3.0	6.2
	Medium	1.4	2.2	7.4
	High	2.8	3.0	5.8
L-curve				
Noise levels in FRFs	Low	4.4	4.3	3.8
	Medium	4.4	4.3	3.7
	High	4.3	4.2	3.8
MFE				
Noise levels in FRFs	Low	0.2	1.6	2.2
	Medium	1.1	1.8	2.2
	High	1.7	2.0	2.3

forces. Again, it is less accurate for low, and to some extent medium, noise level in responses than OCV but better for high noise in the responses.

Very similar results, not presented, were found when the force positions are coincident with the response positions.

In conclusion, the performance of force reconstruction is better when force positions are well separated from each other than when they are close together. However, considerable benefit is obtained by locating response locations close to force positions. In each case OCV gives slightly better results than GCV, although as the results improve the difference between the methods becomes less. In most cases, the L-curve method gives consistent results that are not greatly affected by the choice of positions, and are better than OCV for high noise in the response and worse for low noise.

6. Effect of the signal-to-noise ratios

In this section, the performance of the various methods for determining the regularization parameter is considered for a larger range of the noise levels, that is the S/N ratio of the FRFs and measured operational responses. Moreover, results are shown across the frequency range rather than as a single frequency-averaged result. The original plate configuration and force positions are used. A series of S/N ratios are used between 40 and 10 dB with a step of 1 dB. The S/N ratio of 40 dB corresponds to a low noise level and that of 10 dB

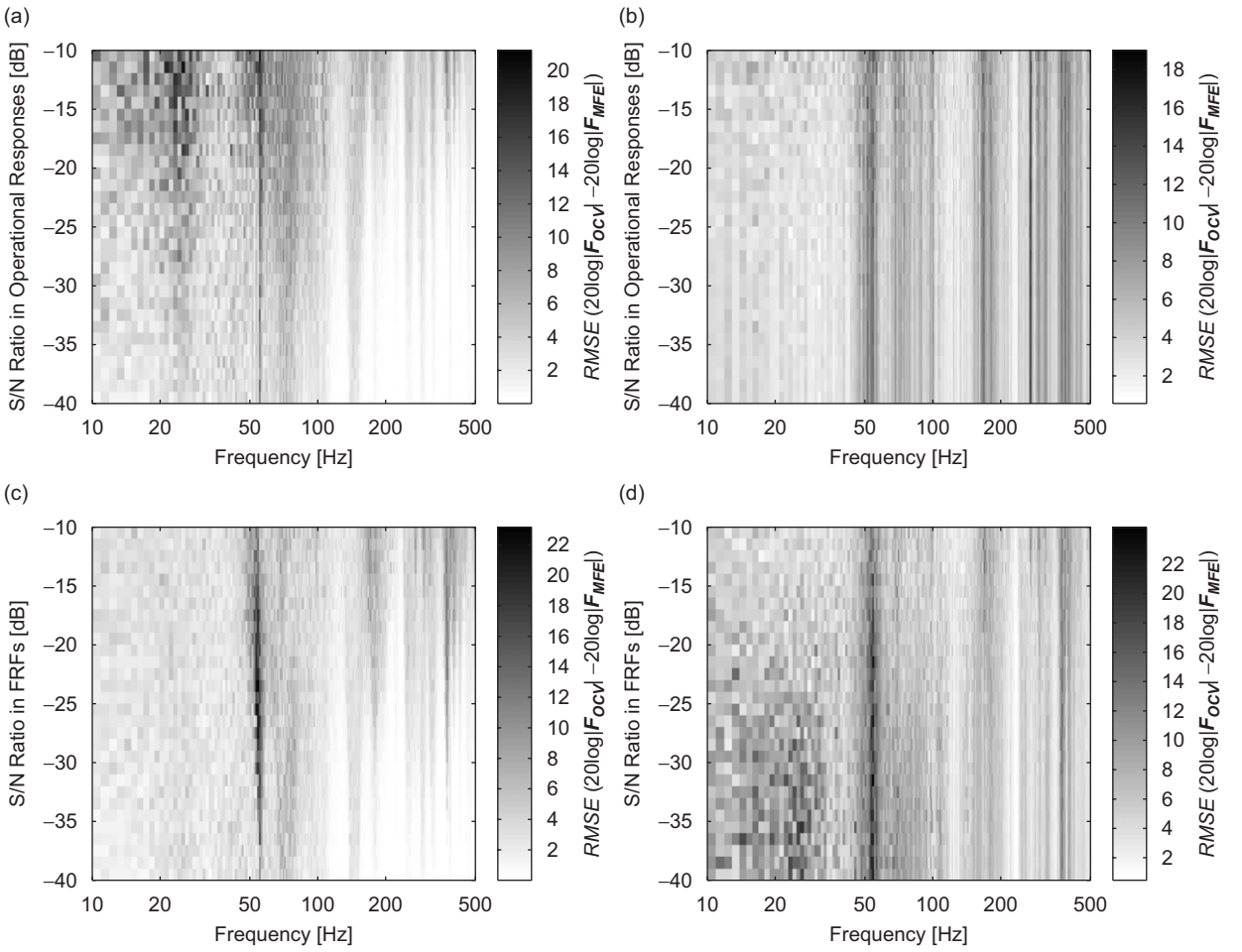

Fig. 12. Average errors in forces reconstructed using OCV. (a) Low noise level in FRFs and variable noise level in operational responses, (b) high noise level in FRFs and variable noise level in operational responses, (c) low noise level in operational responses and variable noise level in FRFs, and (d) high noise level in operational responses and variable noise level in FRFs. RMSE is in dB; dark shading indicates large error, white indicates small error.

corresponds to a high noise level. The noise here differs slightly from that considered in earlier sections by the fact that it is proportional to the signal at every frequency whereas previously it was not, as seen in Fig. 4, the S/N ratios quoted in Table 2 being average values over the frequency range. Note also that only single noise samples are used with random phase, whereas previously averaging was performed in obtaining "measured" FRFs and operational responses. However, 10 sets of results of reconstructed forces and regularization parameters are obtained from 10 different sets of measured frequency response functions and operational responses and the average result from these 10 cases is considered to give some smoothing.

Using the measured frequency response functions and operational responses with S/N ratios of 40 to 10 dB with a step of 1 dB, the average errors of the reconstructed forces are calculated by using each of the methods: OCV, GCV, L-curve and MFE. These were carried out for the following conditions:

(1) low noise level in FRFs, variable noise in operational responses,
(2) high noise level in FRFs, variable noise in operational responses,
(3) low noise level in operational responses, variable noise in FRFs, and
(4) high noise level in operational responses, variable noise in FRFs,

where low noise level is 40 dB S/N ratio and high noise level is 10 dB.

The average errors in the forces are determined as the root mean square error (RMSE) between the forces obtained by OCV (or GCV or L-curve) and the forces obtained by MFE (not the exact forces), which are the

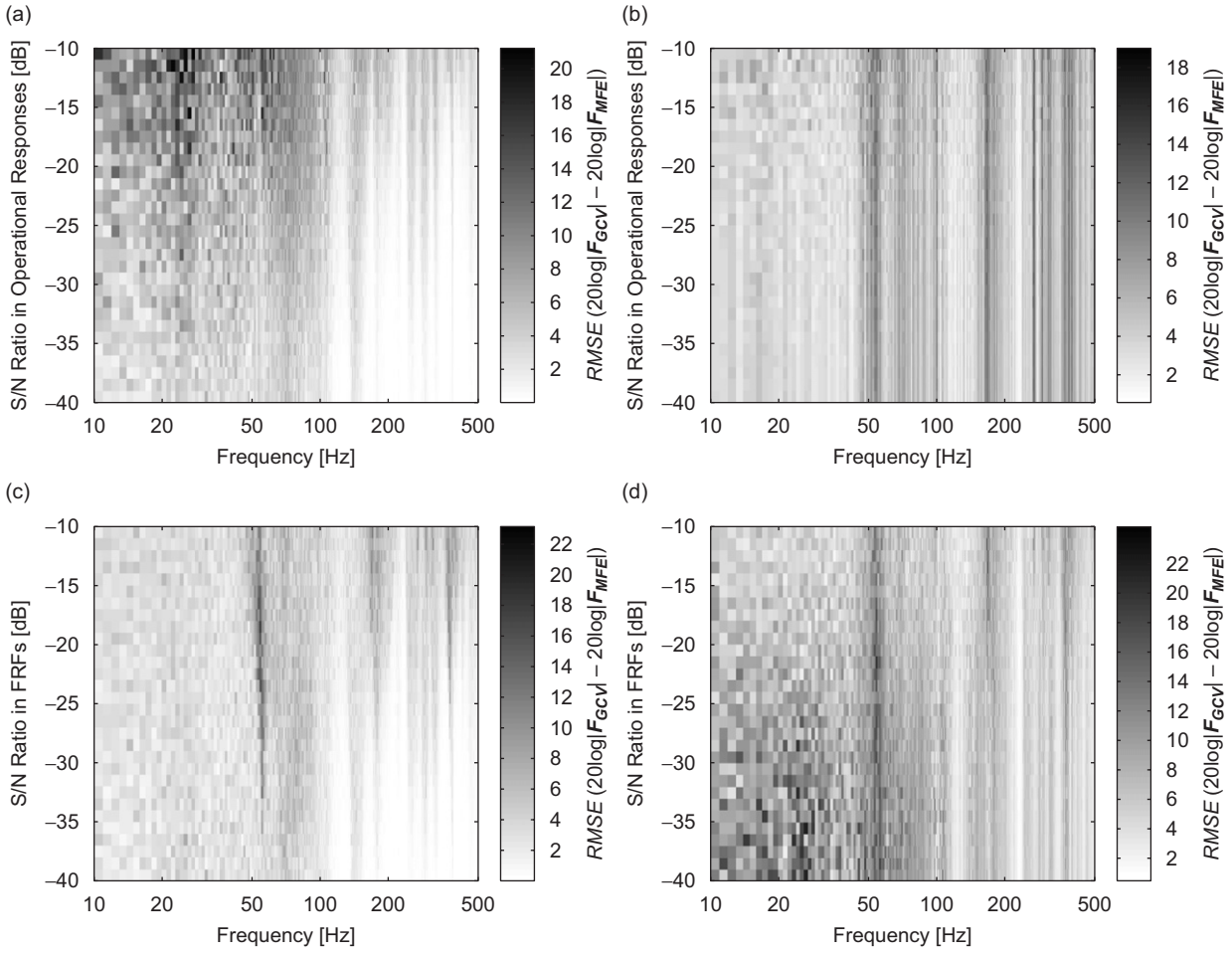

Fig. 13. Average errors in forces reconstructed using GCV. Legend as for Fig. 12.

best that can be achieved by regularization. This may be written as

$$\Delta F_{\text{method}} = \frac{1}{m}\sum_{i=1}^{m}\sqrt{\frac{1}{n}\sum_{j=1}^{n}\left(20\log\left|F^{(i)}_{\text{method},j}\right| - 20\log\left|F^{(i)}_{MFE,j}\right|\right)^2}, \tag{17}$$

where method is OCV, GCV or L-curve, m is the number of result sets (here 10), and n is the number of forces (here 4). Figs. 12–14 show the results for each set of conditions listed above.

Comparing the results for OCV and GCV, Figs. 12 and 13, it can be seen that there are similar trends in each of the conditions. The force errors are small above 100 Hz, where the condition number is small, and in this range the errors are relatively unaffected by noise. For low noise in the FRFs and high noise in the responses there are considerable force errors at low frequencies where the condition numbers are high. It is these errors that tend to dominate the frequency-average results in Table 3.

From a comparison of Figs. 12 and 14 it can be seen that the L-curve method greatly improves the estimates at low frequencies but tends to give a worse estimate for low noise in FRFs between 50 and 100 Hz and to a lesser extent also at high frequencies.

In order to allow a more ready comparison of the results obtained by the three methods, Fig. 15 shows the differences between the average errors in forces obtained by OCV and by GCV and Fig. 16 shows the equivalent comparison between OCV and L-curve. These figures show the area where each method gives the best performance. In order to separate the regions where each method gives better results, the following

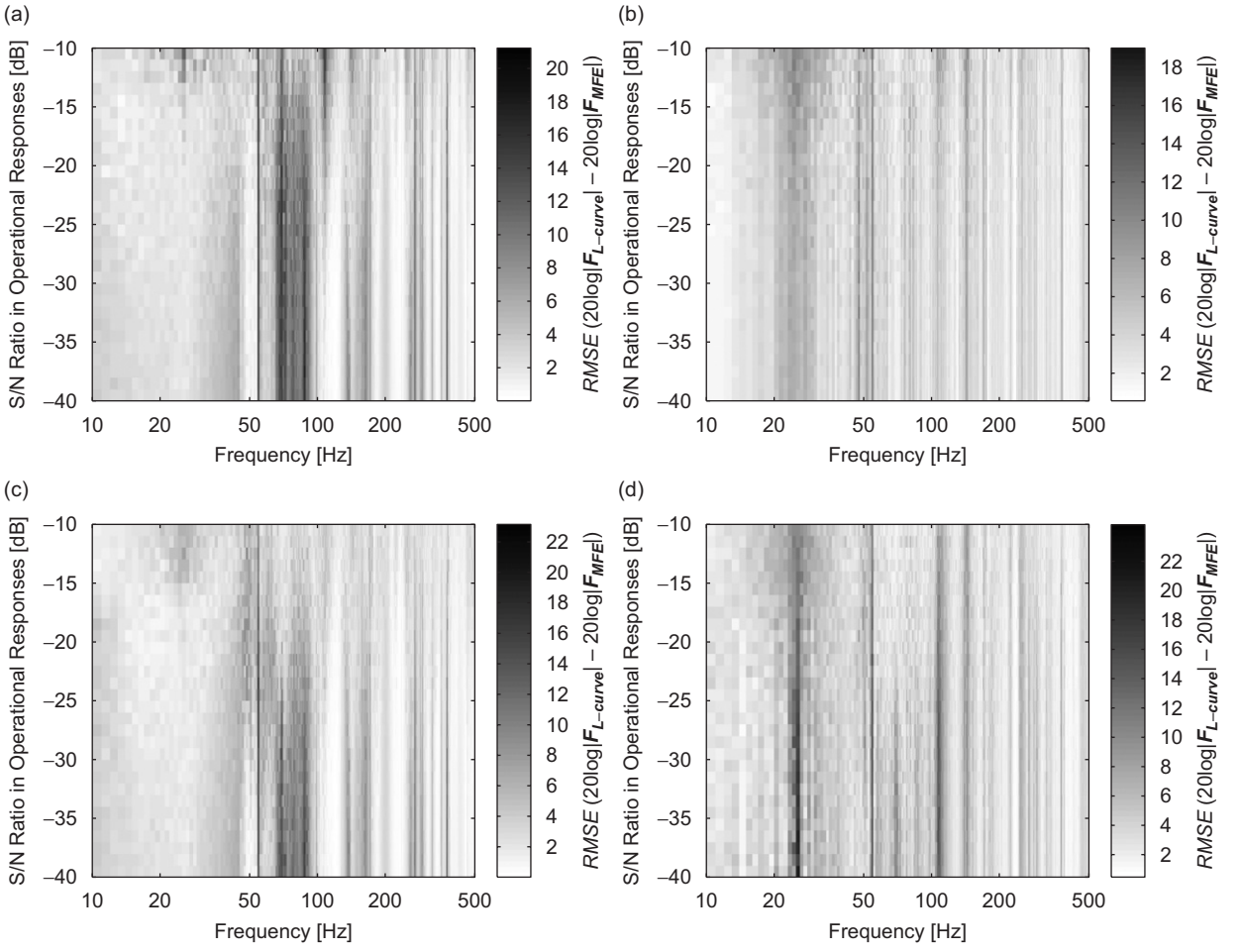

Fig. 14. Average errors in forces reconstructed using L-curve. Legend as for Fig. 12.

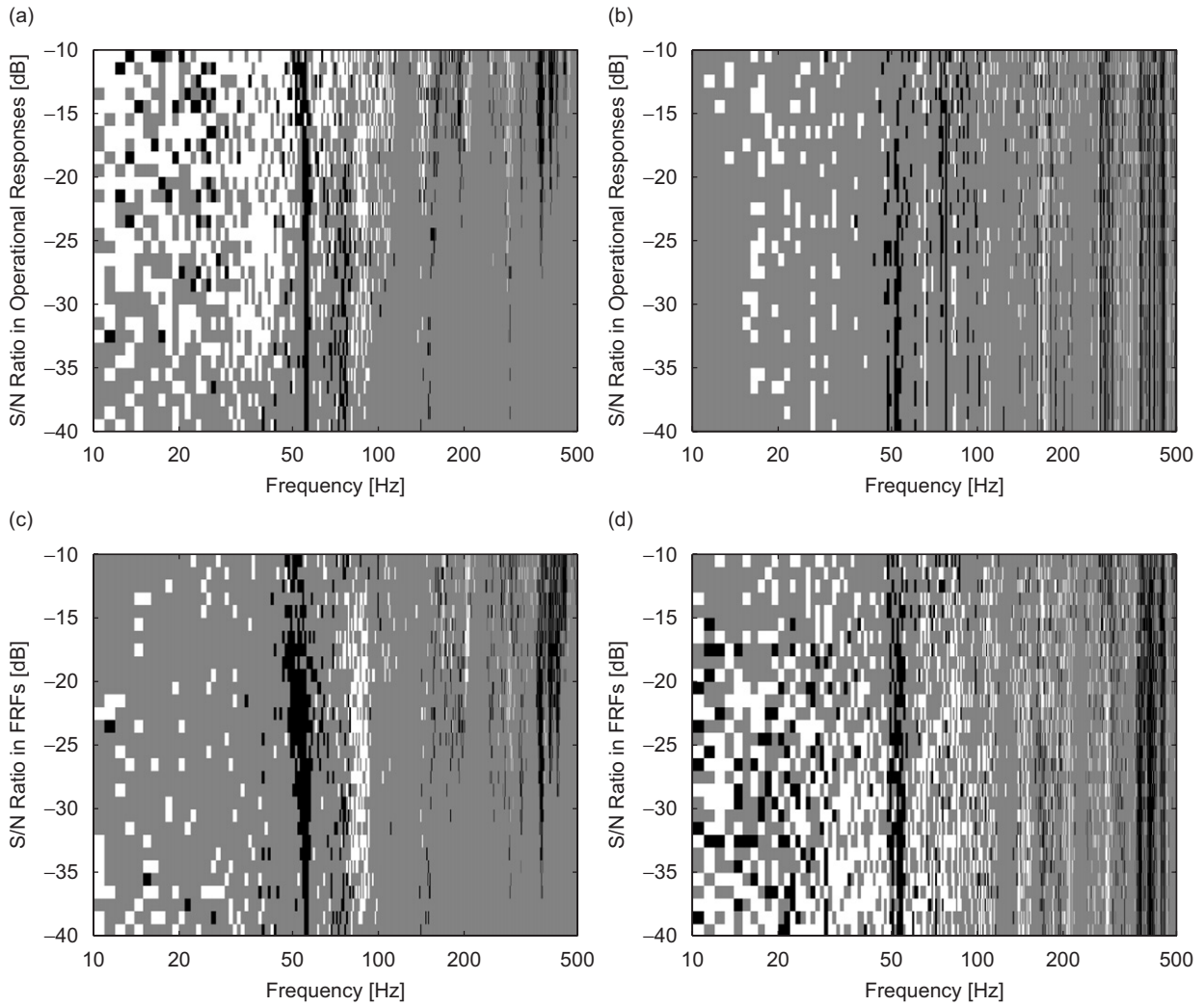

Fig. 15. Comparison of average errors in forces reconstructed by OCV and GCV for various noise levels in operational responses and FRFs. □: OCV better, ▩: OCV and GCV give similar result, ■: GCV better. (a) Low noise level in FRFs and variable noise level in operational responses, (b) high noise level in FRFs and variable noise level in operational responses, (c) low noise level in operational responses and variable noise level in FRFs, and (d) high noise level in operational responses and variable noise level in FRFs.

regions are defined:

$$\begin{aligned} &\text{OCV better}: && \Delta F_{\mathrm{OCV}} - \Delta F_{\mathrm{GCV}} \leqslant -1\,\mathrm{d}B, \\ &\text{Similar}: && |\Delta F_{\mathrm{OCV}} - \Delta F_{\mathrm{GCV}}| < +1\,\mathrm{d}B, \\ &\text{GCV better}: && \Delta F_{\mathrm{OCV}} - \Delta F_{\mathrm{GCV}} \geq +1\,\mathrm{dB}, \end{aligned} \tag{18}$$

and similarly for the comparison of OCV and L-curve. From Fig. 15, OCV is seen to perform better than GCV in the low frequency region below 100 Hz apart from around 50 Hz, and GCV performs better around 50 Hz and above 100 Hz.

From the equivalent comparison between OCV and L-curve in Fig. 16, it can be seen that the trends are more complex. At low frequencies, especially 20–35 Hz where the condition numbers are high, OCV works best when the FRF noise levels are high (Fig. 16(b)) and L-curve works best when they are low (Fig. 16(a)). At higher frequencies, where the condition numbers are low, the reverse trend is found. The worst case for OCV,

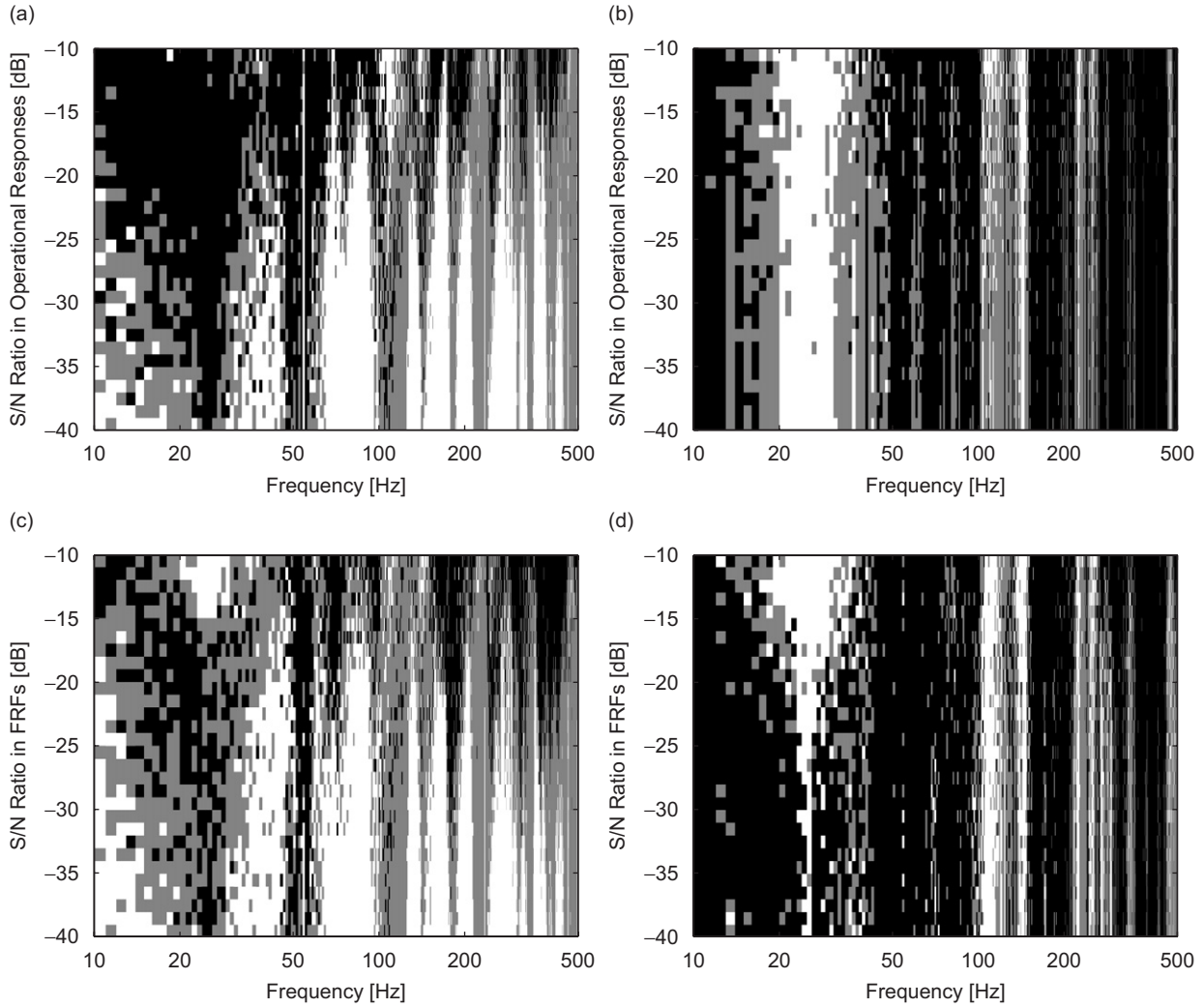

Fig. 16. Comparison of average errors in forces reconstructed by OCV and L-curve for various noise levels in operational responses and FRFs. □: OCV better, ▩: OCV and L-curve give similar result, ■: L-curve better. (a) Low noise level in FRFs; (b) high noise level in FRFs; (c) low noise level in responses; and (d) high noise level in responses.

low noise in FRFs and high noise in responses, can be seen to give better results by L-curve at most frequencies (top of Fig. 16(a) and bottom of Fig. 16(d)). Similarly the best case for OCV, low noise in both FRFs and responses, gives better results by OCV for most frequencies (bottom of Figs. 16(a) and (c)).

Finally, to summarize these results, the average of the results in Figs. 15 and 16 is obtained over frequency. These are first averaged in each one-third octave band and then the average over all one-third octave bands is formed. For calculating this average, for example in the white areas where OCV performs better than GCV a value of $+1$ is taken, in the black areas where GCV performs better than OCV a value of -1 is taken, and the grey is allocated a value of 0. So if the average is positive then OCV performs better than GCV, and if that is negative then GCV performs better than OCV.

Fig. 17 shows the results of this analysis. It can be seen that OCV performs better than or equal to GCV in all cases. It is clearly better than GCV for low noise levels in FRFs and high noise in operational responses. These results are consistent with the previous results in Table 3.

Comparing OCV and L-curve, OCV is clearly better for low noise in FRFs and responses and L-curve is better for high noise in either FRFs or responses.

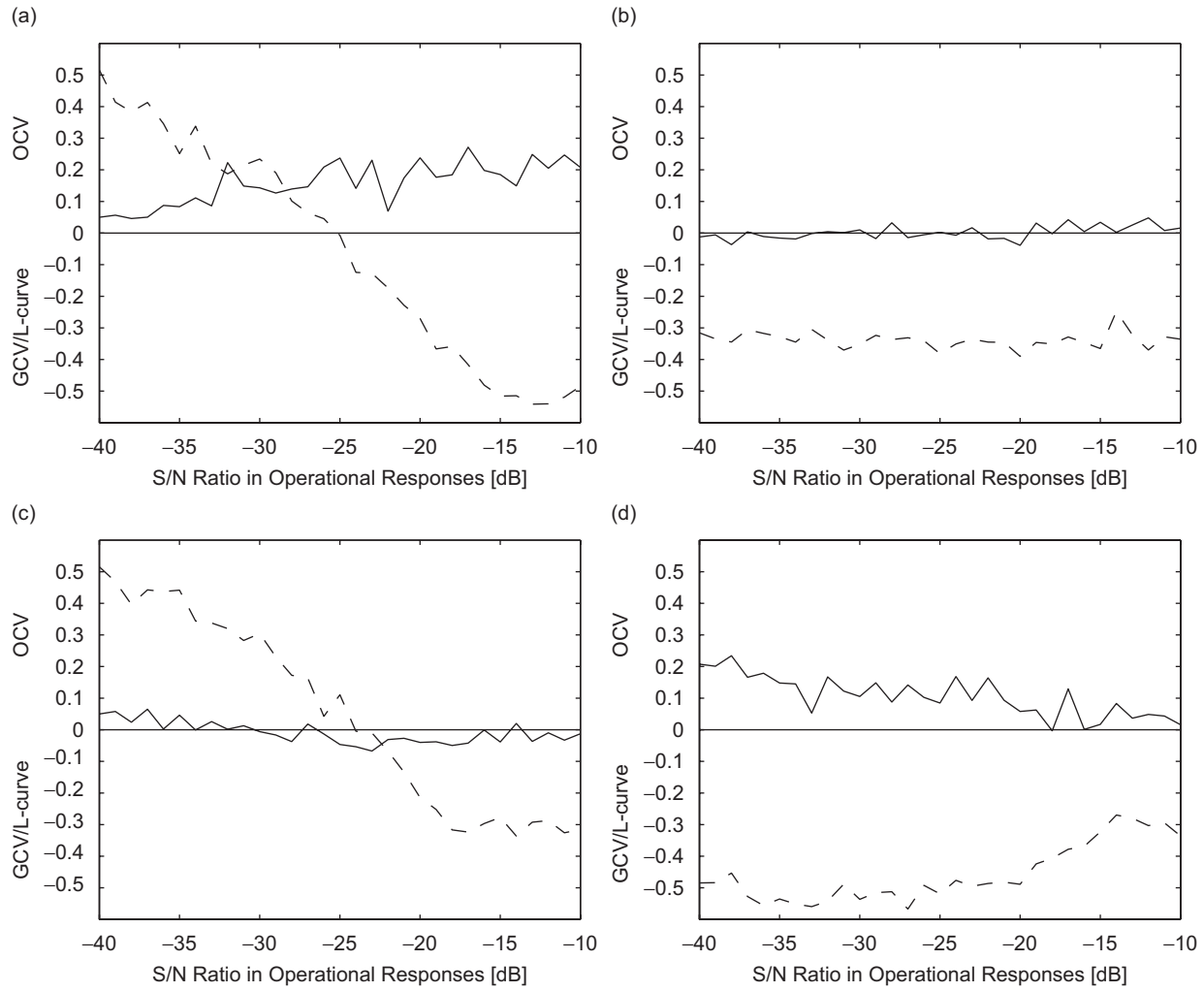

Fig. 17. The average performance of each method calculated in one-third octave bands for various noise levels in operational responses and FRFs. —— OCV compared with GCV, ------ OCV compared with L-curve. (a) Low noise level in FRFs; (b) high noise level in FRFs; (c) low noise level in responses; and (d) high noise level in responses. Values above 0 indicate that OCV gives better results than the other method.

7. Conclusions

The methods of ordinary cross validation, generalized cross validation and L-curve criterion in determining the Tikhonov regularization parameter were compared for application to inverse force determination in structural dynamics.

The L-curve method performs better than OCV or GCV for high noise, particularly in the operational responses, but less well when these noise levels are low. It is therefore less susceptible to large reconstruction errors but it tends to over-regularize the solution in the presence of low noise, leading to under-estimates of the forces. As the operational responses are likely to be contaminated by noise, this suggests that the L-curve method is likely to be the most appropriate method in many practical situations.

It has been seen that the method of OCV generally gives better results than that of GCV. Although GCV was originally introduced to overcome problems that occur with OCV where the matrix to be inverted is near diagonal, such situations have not been encountered in the present study. GCV has only been found to perform better than OCV where condition numbers are lower (corresponding to high frequencies); its

performance is worse than OCV where condition numbers are higher, which is where regularization is more important (at low frequencies). Rather than using GCV, a previously investigated method of only using regularization for condition numbers above a certain threshold seems preferable [14].

The robustness of the conclusions was confirmed for different noise levels in FRFs and in operational responses and for different plate geometries and force locations.

In practice, measurements of FRFs are unlikely to have noise levels as high as 10 dB below the signal. The measurements of operational responses may be more susceptible to noise contamination. It is therefore important to obtain good estimates of the likely noise in the signals before determining the most appropriate regularization technique.

For simplicity the work has been based on a rectangular plate. It is recognized that built-up structures could pose different complexities due to the multi-axial nature of the problem, which may result in difficulties in choosing the number and direction of forces. Built-up structures also result in interaction between different wave types, which cannot be considered in the case of the plate studied. Nevertheless, the techniques which are studied here do not depend on the details of the structure and it is therefore expected that they should perform equally well for any structure, provided that the choice of force and response positions is sufficient to represent the wave fields present in the structure. It is also noted that, by covering a wide frequency range, the study has covered both low and high modal density regions, allowing application to a wide range of problems.

Acknowledgements

This research was supported by the Post-Doctoral Fellowship Program of the Korea Science and Engineering Foundation (KOSEF), Daejeon-City, Korea.

References

[1] J.W. Verheij, Inverse and reciprocity methods for machinery noise source characterization and sound path quantification, part 1: sources, *International Journal of Acoustics and Vibration* 2 (1) (1997) 11–20.
[2] J.W. Verheij, Inverse and reciprocity methods for machinery noise source characterization and sound path quantification, part 2: transmission paths, *International Journal of Acoustics and Vibration* 2 (3) (1997) 103–112.
[3] M.H.A. Janssens, J.W. Verheij, D.J. Thompson, The use of an equivalent forces method for the experimental quantification of structural sound transmission in ships, *Journal of Sound and Vibration* 226 (2) (1999) 305–328.
[4] A.N. Thite, D.J. Thompson, Study of indirect force determination and transfer path analysis using numerical simulations for a flat plate, ISVR Technical Memorandum No. 851, May 2000.
[5] A.N. Thite, Inverse Determination of Structure-borne Sound Sources, Ph.D. Thesis, ISVR, University of Southampton, 2002.
[6] J. Biemond, R.L. Lagendijk, R.M. Mersereau, Iterative methods for image deblurring, *Proceedings of the IEEE* 78 (5) (1990) 856–883.
[7] E. Williams, Regularization and Nearfield Acoustical Holography, *Proceedings of Internoise 2000*, Nice, France, 2000, pp. 73–79.
[8] B.K. Kim, J.G. Ih, Design of an optimal wave vector filter for enhancing the resolution of reconstructed source field by near-field acoustical holography (NAH), *Journal of the Acoustical Society of America* 107 (6) (2000) 3289–3297.
[9] P.A. Nelson, S.H. Yoon, Estimation of acoustic source strength by inverse methods: part I, conditioning of the inverse problem, *Journal of Sound and Vibration* 233 (4) (2000) 643–668.
[10] S.H. Yoon, P.A. Nelson, Estimation of acoustic source strength by inverse methods: part II, experimental investigation of methods for choosing regularization parameters, *Journal of Sound and Vibration* 233 (4) (2000) 669–705.
[11] A.N. Thite, D.J. Thompson, The quantification of structure-borne transmission paths by inverse methods. Part 1: improved singular value rejection methods, *Journal of Sound and Vibration* 264 (2) (2003) 411–431.
[12] A.N. Thite, D.J. Thompson, The quantification of structure-borne transmission paths by inverse methods. Part 2: use of regularization techniques, *Journal of Sound and Vibration* 264 (2) (2003) 433–451.
[13] M. Allen, The relationship between variable selection and data augmentation and a method for prediction, *Technometrics* 16 (1974) 125–127.
[14] H.G. Choi, A.N. Thite, D.J. Thompson, A threshold for the use of Tikhonov regularization in inverse force determination, *Applied Acoustics* 67 (2006) 700–719.
[15] G.H. Golub, M. Heath, G. Wahba, Generalized cross-validation as a method for choosing a good ridge parameter, *Technometrics* 21 (2) (1979) 215–223.
[16] P.C. Hansen, *Rank-Deficient and Discrete Ill-Posed Problems*, SIAM, Philadelphia, 1998.
[17] Y. Kim, P.A. Nelson, Optimal regularisation for acoustic source reconstruction by inverse methods, *Journal of Sound and Vibration* 275 (2004) 463–487.